

Cosmological test of local position invariance from the asymmetric galaxy clustering

Shohei Suga,^{1,*} Atsushi Taruya,^{2,3} Yann Rasera,⁴ and Michel-Andr s Breton^{5,6,7}

¹*Laboratoire Univers et Th ories, Observatoire de Paris,*

Universit  PSL, Universit  de Paris, CNRS, F-92190 Meudon, France

²*Center for Gravitational Physics, Yukawa Institute for Theoretical Physics, Kyoto University, Kyoto 606-8502, Japan*

³*Kavli Institute for the Physics and Mathematics of the Universe (WPI),*

The University of Tokyo Institutes for Advanced Study,

The University of Tokyo, 5-1-5 Kashiwanoha, Kashiwa, Chiba 277-8583, Japan

⁴*Laboratoire Univers et Th ories, Universit  de Paris,*

Observatoire de Paris, Universit  PSL, CNRS, F-92190 Meudon, France

⁵*Aix Marseille Univ, CNRS, CNES, LAM, Marseille, France*

⁶*Institute of Space Sciences (ICE, CSIC), Campus UAB,*

Carrer de Can Magrans, s/n, 08193 Barcelona, Spain

⁷*Institut d'Estudis Espacials de Catalunya (IEEC),*

Carrer Gran Capit  2-4, 08193 Barcelona, Spain

(Dated: December 16, 2021)

The local position invariance (LPI) is one of the three major pillars of Einstein equivalence principle, ensuring the space-time independence on the outcomes of local experiments. The LPI has been tested by measuring the gravitational redshift effect in various depths of gravitational potentials. We propose a new cosmological test of the LPI by observing the asymmetry in the cross-correlation function between different types of galaxies, which predominantly arises from the gravitational redshift effect induced by the gravitational potential of halos at which the galaxies reside. We show that the ongoing and upcoming galaxy surveys can give a fruitful constraint on the LPI-violating parameter, α , at distant universes (redshift $z \sim 0.1 - 1.8$) over the cosmological scales (separation $s \sim 5 - 10 \text{ Mpc}/h$) that have not yet been explored, finding that the expected upper limit on α can reach 0.03.

Introduction.— Since its foundation, general relativity has been the essential framework to describe gravity in astronomy and cosmology. An important building block of general relativity is the Einstein equivalence principle, and as part of the Einstein equivalence principle, the local position invariance (LPI) has been playing a special role even for alternative theories of gravity. It states that the outcome of any local non-gravitational experiment is independent of where and when it is performed. An important consequence of the LPI is the prediction of the gravitational redshift effect. It indicates that the gravitational redshift, z_{grav} , between two identical clocks located at different gravitational potential, $\Delta\phi$, can be given by $z_{\text{grav}} = \Delta\phi$ (we are working with units of the speed of light being unity, $c = 1$). However, if the LPI is violated, this relation has to be modified, and it is commonly parametrized in the form (e.g., Ref. [1]):

$$z_{\text{grav}} = (1 + \alpha)\Delta\phi, \quad (1)$$

where the non-zero value of α implies the violation of LPI.

Refs. [2, 3] have made the first successful high-precision measurements of the gravitational redshift effect due to the gravitational potential of the Earth (so-called the Pound-Rebka-Snider experiment), constraining the LPI-violating parameter with an accuracy of $\alpha \lesssim O(10^{-2})$. After these pioneering works, the constraint on α has been obtained and improved by many measurements, for instance, spacecraft measurements [4, 5], solar spectra

measurements [6, 7], and null redshift experiments, which constrain the difference in α between different kinds of atomic clocks in the laboratory [8, 9]. Recent null redshift experiment puts the upper bound on the LPI-violating parameter by $\alpha < O(10^{-6})$ [9]. The limits on α obtained above works cover a range of $10^{-15} \lesssim \Delta\phi \lesssim 10^{-6}$. Interestingly, Refs. [10, 11] have recently measured the stellar/quasar spectrum near the galactic centre supermassive black hole and gave a limit on a violation of the LPI of $\alpha \lesssim 10^{-2}$ with a potential difference $\Delta\phi \approx 10^{-4} - 10^{-2}$.

In this *Letter*, we propose a novel cosmological test of the LPI by using the measurements of galaxy redshift surveys. The observed galaxy distributions via spectroscopic measurement are apparently distorted due to the special and general relativistic effects (e.g., Refs. [12–18]). Some of the relativistic effects induce asymmetric distortions along a line-of-sight direction, and taking a cross-correlation between different types of galaxies, this leads to the non-vanishing dipole moment.

Refs. [19, 20] have studied the dipole signal at large scales, and pointed out that it would be useful to test the weak equivalence principle. On the other hand, based on the numerical simulations and analytical model, we have recently shown that the signal at small scales is dominated by the gravitational redshift effect mainly arising from the gravitational potential of dark matter halos [21, 22]. In the companion paper [23], we have shown that the upcoming galaxy surveys would detect the dipole

anisotropy at a statistically significant level (see Ref. [24] for a similar forecast based on a different perturbative approach). Note that even the current data set provides a marginal detection not only from galaxy clustering [25] but also from clusters of galaxies [26–29]. We thus anticipate that the detected dipole signals from future surveys enable us to measure the gravitational redshift effect, offering the LPI test at cosmological scales.

Motivated by these, we here present a quantitative analysis for the forecast constraint on the LPI-violating parameter α . In doing so, we use the analytical model which reproduces numerical simulations quite well [22, 23]. Taking also two major systematics arising from off-centered galaxies into account, we demonstrate that future galaxy surveys will offer an insightful test of the LPI, uncovering the parameter space that has not been so far explored.

Relativistic dipole.— Let us recall that the observed galaxy position via spectroscopic surveys receives relativistic corrections through the light propagation in an inhomogeneous universe on top of the cosmic expansion. As a result, the observed source position, \mathbf{s} , differs generally from the true position, \mathbf{x} . Taking the major effects into account, their relation becomes

$$\mathbf{s} = \mathbf{x} + \frac{1}{aH} \left[(\mathbf{v} \cdot \hat{\mathbf{x}}) - \phi_{\text{halo}} + \frac{v_g^2}{2} \right] \hat{\mathbf{x}}, \quad (2)$$

where $\hat{\mathbf{x}}$ is the unit vector defined by $\hat{\mathbf{x}} = \mathbf{x}/|\mathbf{x}|$ and a , H , and \mathbf{v} are a scale factor, Hubble parameter, and peculiar velocity of galaxies, respectively. The explicit form of other minor contributions can be found in the literature (e.g., Refs. [30–32]). In Eq. (2), we describe three contributions in the square bracket of the right-hand side as follows: from the first to third terms, (i) the longitudinal Doppler effect induced by the peculiar motion of galaxy, (ii) gravitational redshift effect arising from the potential at the galaxy position, dominantly attributed to the halo potential¹, ϕ_{halo} , and finally, (iii) transverse Doppler effect mainly due to the virialized random motion of the galaxy, v_g^2 . Since the second and third terms largely depend on the halo properties of targeted galaxies, they are systematically treated as a deterministic constant rather than the stochastic variable, determined solely by the halo masses. In Eq. (2), relativistic corrections systematically change the observed position along the specific direction $\hat{\mathbf{x}}$. This can apparently produce an asymmetry in the galaxy clustering, and taking a pair of galaxies with different sizes of relativistic corrections

results in a non-vanishing dipole moment, as we will see below.

Through the mapping relation in Eq. (2), the number density fluctuation of the observed galaxies, $\delta(\mathbf{s})$, is linked to the quantities defined in the real space, and treating these quantities and relativistic corrections perturbatively, we obtain [23]

$$\begin{aligned} \delta(\mathbf{s}) = & \int \frac{d^3 \mathbf{k}}{(2\pi)^3} e^{i\mathbf{k} \cdot \mathbf{s}} \left[\left(b + f\mu_k^2 - if\frac{2}{ks}\mu_k \right) \delta_L(\mathbf{k}) \right. \\ & - \frac{1}{saH} \left(\phi_{\text{halo}} - \frac{v_g^2}{2} \right) \left\{ -1 + (1-2f)\mu_k^2 \right. \\ & \left. \left. - i(1+f)\frac{2}{ks}\mu_k - ibks\mu_k - ifks\mu_k^3 \right\} \delta_L(\mathbf{k}) \right], \quad (3) \end{aligned}$$

where the quantity $\delta_L(\mathbf{k})$ is the Fourier transform of the linear matter density field. The quantity μ_k is the directional cosine defined by $\mu_k \equiv \hat{\mathbf{s}} \cdot \hat{\mathbf{k}}$, and the function f is the linear growth rate given by $f \equiv d \ln D / d \ln a$, with D being the linear growth factor. Note that the galaxy distribution is in general a biased tracer of large-scale matter density fluctuations, and in deriving Eq. (3), the real-space galaxy density field was assumed to be linearly proportional to δ_L , introducing the proportional constant b called the linear bias parameter, which must be determined observationally. In the first line, the terms having an explicit μ_k -dependence are induced by the Doppler effect [33]. On the other hand, second and third lines arise from the gravitational redshift and transverse Doppler effects, with major contributions coming from halos hosting the observed galaxies.

Using Eq. (3), we compute the two-point cross-correlation function between the objects X at \mathbf{s}_1 and Y at \mathbf{s}_2 , by taking the ensemble average: $\xi_{XY}(s, d, \mu) \equiv \langle \delta_X(\mathbf{s}_1) \delta_Y(\mathbf{s}_2) \rangle$. Here, we express the two-point cross-correlation as a function of the separation $s = |\mathbf{s}_2 - \mathbf{s}_1|$, line-of-sight distance $d = |(\mathbf{s}_1 + \mathbf{s}_2)/2|$, and directional cosine between the line-of-sight and separation vectors, $\mu = \hat{\mathbf{s}} \cdot \hat{\mathbf{d}}$. To quantify the asymmetry in the galaxy clustering, we introduce the dipole moment of the two-point correlation function, which is defined by $\xi_{XY,1}(s, d) = \frac{3}{2} \int_{-1}^1 d\mu \mu \xi_{XY}(s, d, \mu)$.

As long as we consider the dipole cross-correlation at a small separation of $s \sim 5\text{--}30 \text{ Mpc}/h$ in the distant universe, the terms of the order of $O((s/d)^2)$ can be ignored. Then, the non-zero contributions to the dipole moment are given by (see Appendix C in Ref. [22] for other mul-

¹ In principle, there exists the contribution from the linear-order density field. While this could be important to probe the equivalence principle at large scales, such a term produces a negligible amount of the gravitational redshift at the scales of our interest, and hence we ignore it.

tipoles)

$$\begin{aligned} \xi_{XY,1}(s, d) &= 2f\Delta b \frac{s}{d} \left(\Xi_1^{(1)} - \frac{1}{5}\Xi_2^{(0)} \right) \\ &+ \frac{1}{saH} \left(\Delta\phi - \frac{\Delta v_g^2}{2} \right) \\ &\times \left(b_X b_Y + \frac{3}{5}(b_X + b_Y)f + \frac{3}{7}f^2 \right) \Xi_1^{(-1)}, \quad (4) \end{aligned}$$

with the function $\Xi_\ell^{(n)}$ defined by

$$\Xi_\ell^{(n)}(s) \equiv \int \frac{k^2 dk}{2\pi^2} \frac{j_\ell(ks)}{(ks)^n} P_L(k), \quad (5)$$

where the functions j_ℓ and $P_L(k)$ are, respectively, the spherical Bessel function and the power spectrum of the linear density fields defined by $\langle \delta_L(\mathbf{k})\delta_L(\mathbf{k}') \rangle = (2\pi)^3\delta_D(\mathbf{k} + \mathbf{k}')P_L$. In Eq. (4), all terms are proportional to the differential quantities, i.e., $\Delta b \equiv b_X - b_Y$, $\Delta\phi \equiv \phi_{\text{halo},X} - \phi_{\text{halo},Y}$, and $\Delta v_g^2 \equiv v_{g,X}^2 - v_{g,Y}^2$. Accordingly, the non-vanishing dipole arises only when we cross-correlate different biased objects, $X \neq Y$. In Eqs. (3) and (4), we ignore the magnification bias that comes from the fact that galaxy samples are flux limited. As shown in Saga *et al.* [23], as long as we focus on small scales of our interest, its effect on the dipole signal is small and does not change the following results.

Given the linear matter power spectrum and bias parameters, the remaining pieces to be specified for a quantitative prediction of $\xi_{XY,1}$ are ϕ_{halo} and v_g^2 , which are modeled by the universal halo density profile, called Navarro-Frenk-White profile [34]. Assuming its functional form characterized by halo mass and redshift, the halo potential, ϕ_{halo} , is obtained by solving the Poisson equation, while the velocity dispersion, v_g^2 , is computed from the Jeans equation [22, 23]. Here, we also add the coherent motion of halos to v_g^2 , following the Gaussian linear density fields (e.g., Refs. [35–37]). In predicting the dipole, a crucial aspect is that each of the galaxies to cross-correlate does not strictly reside at the halo center, and the presence of the off-centered galaxies induces two competitive effects, i.e., the diminution of the gravitational redshift and non-vanishing transverse Doppler effects, which can systematically change the dipole amplitude. We account for these following Refs. [38, 39], and control their potential impact by introducing the off-centering parameter R_{off} .

Putting all ingredients together, we demonstrate the analytical prediction of the dipole in Fig. 1, where we show the results at $z = 0.33$, together with the measured dipole in simulations incorporating longitudinal Doppler and gravitational redshift effects (black circles), and all the relevant relativistic effects (grey circles) [21]. Comparing black and grey circles with errorbars confirms that the longitudinal Doppler and gravitational redshift effects are the major contributors to the dipole, and accordingly, it justifies the underlying assumption in our

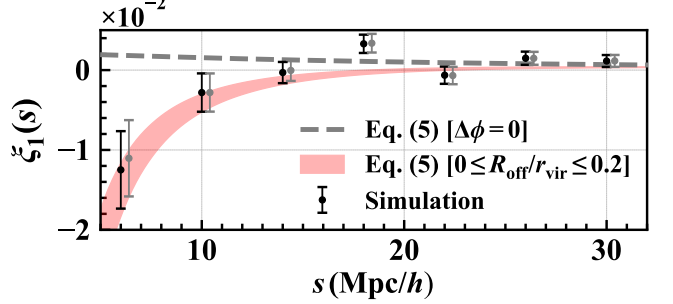


FIG. 1. Dipole moment cross-correlating $b_X = 2.07$ and $b_Y = 1.08$ at $z = 0.33$ based on our model with varying $0 \leq R_{\text{off}}/r_{\text{vir}} \leq 0.2$ (red shaded curve). In the red shaded curve, the lower and upper lines correspond to $R_{\text{off}}/r_{\text{vir}} = 0$ and 0.2 , respectively. The grey dashed line represents the analytical prediction neglecting the halo potential, $\Delta\phi_{\text{halo}}$. The circles with errorbars represent the simulation results taking both Doppler and gravitational redshift effects (black) and all relevant relativistic effects (grey) [22], whose errorbars are estimated by using the jackknife method. Note that the grey data points are artificially shifted for presentation purposes.

model given in Eq. (4). In this figure, we vary the off-centering parameter by the typical range for the simulations, i.e., the offset of the deepest potential well from the center of mass position which is the actual halo position defined in simulations: $0 \leq R_{\text{off}}/r_{\text{vir}} \leq 0.2$ (see e.g., Ref. [39]). Within the statistical error, the prediction depicted as a red shaded curve describes the simulation results remarkably well down to $5 \text{ Mpc}/h$, while the prediction ignoring the halo potential (grey dashed) fails to reproduce the negative dipole at small scales. This suggests that the measurements of the dipole moment, having particularly a negative amplitude at $s \lesssim 30 \text{ Mpc}/h$, provide us with the information about the gravitational redshift effect from the halo potential, which can be used to test/constrain the LPI violation, as we will see in the next section.

Test of Local Position Invariance.— Having confirmed that the analytical predictions properly describe the dipole signal at the scales of our interest, we next consider quantitatively the prospects for constraining the LPI-violation parameter α in Eq. (1) from upcoming galaxy surveys.

To this end, we perform the Fisher matrix analysis involving several parameters together with α as follows.

- *cosmological parameters*: the cosmological parameters that characterize the linear matter spectrum P_L and growth of structure are assumed to be determined by other cosmological probes e.g., cosmic microwave background (CMB) observations, and we fix their fiducial values to the seven-year WMAP results [40].

- *bias parameter*: the redshift-space distortions and

baryon acoustic oscillations measurements provide the constraint on $b\sigma_8$ with σ_8 being the fluctuation amplitude smoothed at $8 \text{ Mpc}/h$. Combining the accurate CMB measurement for power spectrum normalization, we thus have the bias b with a certain error, σ_b (see e.g., Refs. [41, 42]). We obtain the error by performing another Fisher analysis for these observations.

On top of these parameters that can be determined independently of the dipole moment, our theoretical template based on Eq. (4) involves parameters associated with the properties of halos for a given redshift:

- *off-centering parameter R_{off}* : in principle, this parameter can be determined separately and accurately from the even multipole moments of ξ_{XY} (e.g., Ref. [38]). Here, we set the typical value of $0.2r_{\text{vir}}$ as a fiducial value, and impose the Gaussian prior with the expected errors $\sigma_{R_{\text{off}}} = 0.01r_{\text{vir}}$, where r_{vir} is the virial radius of halos (see e.g., Refs. [38, 39, 43]).
- *halo mass*: the halo masses $M_{X/Y}$ are assumed to be inferred from the bias parameters with errors, $\sigma_M = |\partial M / \partial b| \sigma_b$, through the bias model described by e.g., the Sheth-Tormen prescription [44]. We incorporate this error into our analysis as a Gaussian prior. Thanks to this assumption, the degeneracy between the LPI-violating parameter, α , and potential difference, $\Delta\phi$, are broken, as seen in Eq. (1). The systemic impact of assuming a specific bias model would be reduced, once the halo masses can be determined by a complementary probe, e.g., gravitational lensing measurements.

To sum up, we have five free parameters in the theoretical template, i.e., $\theta_i = \{\alpha, R_{\text{off},X/Y}, \text{ and } M_{X/Y}\}$. With the prescription given above, the test of LPI proposed here will be performed under consistency with the standard cosmological model.

Let us construct the 5×5 Fisher matrix for the n th redshift bin of assuming surveys by

$$F_{n,ij} = \sum_{s_1, s_2 = s_{\min}}^{s_{\max}} \frac{\partial \xi_{XY,1}(s_1, z_n)}{\partial \theta_i} \times \text{COV}^{-1}(s_1, s_2, z_n) \frac{\partial \xi_{XY,1}(s_2, z_n)}{\partial \theta_j}, \quad (6)$$

where the function $\text{COV}(s_1, s_2, z_n)$ represents the covariance matrix, which is analytically evaluated by taking only the dominant plane-parallel contributions, ignoring also the non-Gaussian contribution. (see Refs. [23, 45, 46] for the explicit form). The minimum separation is set to be $s_{\min} = 5 \text{ Mpc}/h$, above which the analytical prediction reproduces the simulations, and we expect to avoid the systematics of baryonic effects that will be addressed in

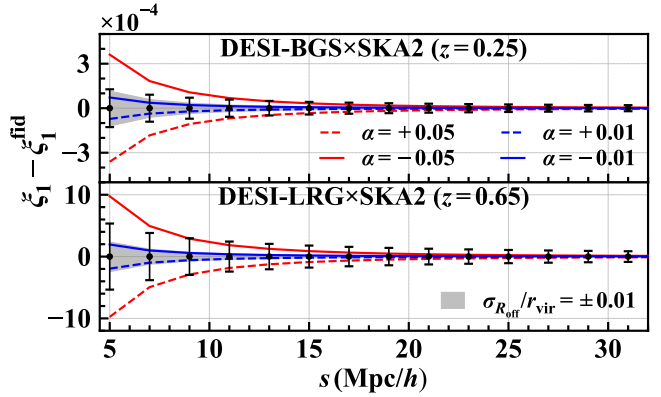


FIG. 2. Expected 1σ error on the dipole around the fiducial signal, i.e., $R_{\text{off}}/r_{\text{vir}} = 0.2$ and $\alpha = 0$, for the future surveys as indicated. The red and blue lines represent the difference between the fiducial signal and the one when $\alpha = \pm 0.05$ and ± 0.01 , respectively. The grey region represents the variation of the signal when varying the off-centering parameter within the prior range, $\sigma_{R_{\text{off}}}/r_{\text{vir}} = \pm 0.01$.

the future work using cosmological hydrodynamic simulations. On the other hand, we set s_{\max} to $30 \text{ Mpc}/h$, below which the gravitational redshift effect from the halo potential starts to be dominated, and adopting a larger value of s_{\max} hardly change the results. Then, with the inverse Fisher matrix for the n th redshift bin of surveys, $\sigma_n^2 \equiv F_{n,\alpha\alpha}^{-1}$, we combine all the redshift bin by $\sigma_\alpha = 1/\sqrt{\sum_n \sigma_n^{-2}}$, which gives the expected 1σ error for a given survey on the LPI-violating parameter α , marginalizing over other parameters.

In the Fisher matrix analysis presented here, we consider the cross-correlation between two distinct biased galaxies obtained from different surveys, assuming that these surveys are maximally overlapped. We examine the combination of the following surveys: Dark Energy Spectroscopic Instrument (DESI) targeting magnitude-limited Bright Galaxies (BGS), Luminous Red Galaxies (LRGs), and Emission Line Galaxies (ELGs) [47], Euclid targeting $\text{H}\alpha$ emitters [48], Subaru Prime Focus Spectrograph (PFS) targeting OII ELGs [49], and Square Kilometre Array (SKA) targeting HI galaxies with two phases dubbed SKA1 and SKA2 [50] (see Appendix E of Ref. [23] for the information on survey parameters). Note that splitting galaxies obtained from a single survey into two subsamples and cross-correlating between them would also yield a non-zero dipole moment. However, its detectability strongly depends on how we split the sample (see Ref. [23]). In this *Letter*, we do not consider the situation involving such uncertainty, and instead focus on a solid way that combines two observations without splitting samples.

For illustration, Fig. 2 presents the expected errors of the dipole signal, around the predictions from the fidu-

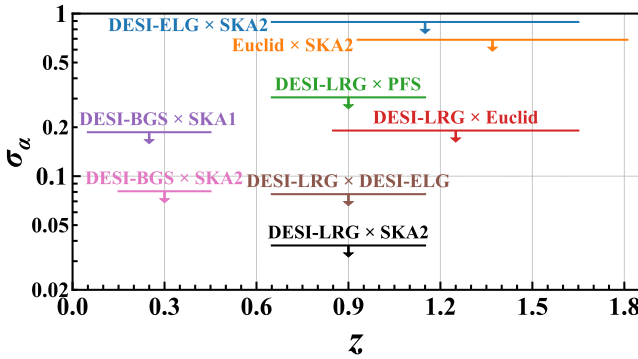


FIG. 3. Expected 1σ error on the LPI-violating parameter α , obtained by cross-correlating different sources observed in different surveys as indicated. The length of each horizontal line represents the survey redshift ranges to obtain the 1σ error.

cial setup (i.e., $R_{\text{off}}/r_{\text{vir}} = 0.2$ and $\alpha = 0$) for DESI-BGS \times SKA2 (*top*) and DESI-LRG \times SKA2 (*bottom*), at the specific redshifts of $z = 0.25$ and $z = 0.65$, respectively. Here, we also show the expected signals when changing the LPI-violating parameter to $\alpha = \pm 0.01$ and 0.05 , and varying the off-centering parameter within the prior range $\sigma_{R_{\text{off}}}/r_{\text{vir}} = 0.01$. Fig. 2 suggests that the dipole signal from upcoming surveys has a potential to detect a violation of the LPI of the order of $\mathcal{O}(\alpha) = 0.01$ even for a single redshift slice if the other parameters are held fixed.

Computing the Fisher matrix, we obtain the 1σ error on the LPI-violating parameter α , with other parameters marginalized over. In Fig. 3, results from various combinations of upcoming surveys are plotted against the redshift. Among these, the combination of DESI-LRG and SKA2 gives the tightest constraint with $\sigma_\alpha \approx 0.037$ at $0.7 \lesssim z \lesssim 1.1$. This is attributed to the large bias difference Δb , increasing the signal, and a large number of galaxies in SKA2, reducing the shot noise. Assuming that all the observations shown in Fig. 3 are independent and combining these upper limits, the LPI-violating parameter is expected to be constrained down to $\sigma_\alpha \approx 0.029$.

In Fig. 4, the cosmological LPI test proposed here is compared to the upper limits on α that have been previously obtained, plotted as a function of measured potential difference $\Delta\phi$. Different colors and symbols indicate methods/experiments to measure the gravitational redshift effects. From Fig. 4, several noticeable points are in order: (i) the dipole measurement can be a unique probe to explore a new parameter space of the LPI violation, i.e., $\Delta\phi \approx 10^{-5}$, (ii) our method is a new approach that cannot be categorized as any previous method, and (iii) the method enables us to, for the first time, constrain the LPI violation at cosmological scales.

Summary and discussions.— To conclude, in this *Let-*

ter, we have explicitly shown that the cross-correlation between galaxies with different host halos and clustering bias yields the non-vanishing dipole moment having a negative amplitude. Such a feature typically appears at $s \lesssim 30 \text{ Mpc}/h$, and is dominated by the gravitational redshift effect from the potential of halos hosting observed galaxies. The analytical model predictions combining the perturbation theory with halo model prescription agree well with simulations taking the relativistic effects into account. The Fisher matrix analysis based on the analytical model showed that despite the systematics arising from the off-centered galaxies, the dipole moment measured from the upcoming galaxy surveys offers a unique test of the LPI at cosmological scales in the high-redshift universes. While the achievable precision of the LPI-violating parameter, $\alpha \lesssim 0.029$, is comparable to the upper limit from the Pound-Rebka-Snider experiments [2, 3] and is weaker than the recent tests based on the null experiments, the proposed method allows us to probe the potential depth of $\Delta\phi \approx 10^{-5}$, which has not been fully explored (Fig. 4).

Finally, the outcome of our Fisher matrix analysis relies on several simplifications and specific setups. Among these, our theoretical template adopts the halo model prescription assuming the one-to-one correspondence between galaxy and halo, and hence the predicted amplitude of the dipole signal is tightly linked to the halo mass. More careful modeling based on numerical simulations is thus required toward future measurements, taking a proper account of the realistic halo-galaxy connection as well as systematic effects from the assembly bias characterizing the secondary halo properties. Another concern would be the impact of off-centered galaxies. While our setup of the off-centering parameter and its Gaussian prior is considered to be reasonable for luminous red and bright galaxies, upcoming surveys will also observe the emission-line galaxies, whose properties might not be necessarily the same. Nevertheless, even with a conservative choice of $R_{\text{off}}/r_{\text{vir}} = 0.4$ and a weak prior condition $\sigma_{R_{\text{off}}}/r_{\text{vir}} = 0.1$, the degradation of the constraint on α is found to be moderate, and we can still perform a meaningful LPI test, with the LPI-violation parameter constrained to be $\alpha \lesssim 0.046$. With given data in the future survey, implementing our model for the likelihood analysis and combining other probes to vary all the relevant parameters, one can expect to obtain a robust constraint on the LPI violation. Hence, a pursuit of measuring the dipole moment is indispensable and the present method will pave a pathway to the cosmological LPI test in the distant universe.

Acknowledgements.— This work was initiated during the invitation program of JSPS Grant No. L16519. Numerical simulation was granted access to HPC resources of TGCC through allocations made by GENCI (Grand Equipement National de Calcul Intensif) under the allocations A0030402287, A0050402287, A0070402287

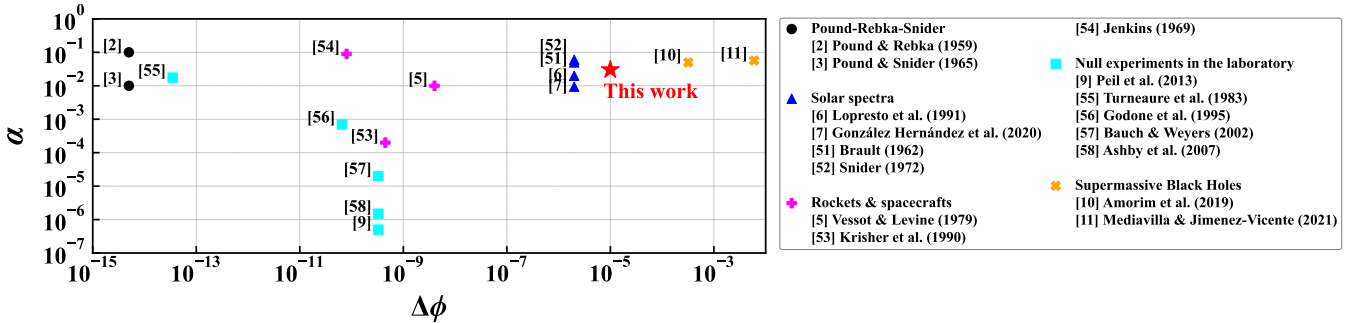


FIG. 4. Upper limits on the LPI-violating parameter α as a function of the difference of gravitational potentials by Pound-Rebka-Snider experiments [2, 3], solar spectra measurements [6, 7, 51, 52], rockets and spacecraft experiments [5, 53, 54], null experiments [9, 55–58], and observations of stars/quasars near the galactic center supermassive black hole [10, 11] as indicated in the right table. (This figure is a reproduction of the original one proposed in Ref. [10], with our results added.)

and A0090402287. Numerical computation was also carried out partly at the Yukawa Institute Computer Facility. This work was supported by Grant-in-Aid for JSPS Fellows No. 17J10553 (SS) and in part by MEXT/JSPS KAKENHI Grant Numbers Nos. JP17H06359, JP20H05861, and 21H01081 (AT). AT also acknowledges the support from JST AIP Acceleration Research Grant No. JP20317829, Japan. SS acknowledges the support from Yukawa Institute for Theoretical Physics (YITP) at Kyoto University, where this work was completed during the visiting program. Also, discussions during the workshop YITP-T-21-06 on “Galaxy shape statistics and cosmology” were useful to complete this work.

[9] S. Peil, S. Crane, J. L. Hanssen, T. B. Swanson, and C. R. Ekstrom, Phys. Rev. A **87**, 010102 (2013), arXiv:1301.6145 [physics.atom-ph].

[10] A. Amorim *et al.* (GRAVITY), Phys. Rev. Lett. **122**, 101102 (2019), arXiv:1902.04193 [astro-ph.GA].

[11] E. Mediavilla and J. Jiménez-Vicente, ApJ **914**, 112 (2021), arXiv:2106.11699 [astro-ph.CO].

[12] M. Sasaki, MNRAS **228**, 653 (1987).

[13] T. Matsubara, ApJ **537**, L77 (2000), arXiv:astro-ph/0004392 [astro-ph].

[14] R. A. C. Croft, MNRAS **434**, 3008 (2013), arXiv:1304.4124 [astro-ph.CO].

[15] J. Yoo, Classical and Quantum Gravity **31**, 234001 (2014), arXiv:1409.3223 [astro-ph.CO].

[16] V. Tansella, C. Bonvin, R. Durrer, B. Ghosh, and E. Selentin, J. Cosmology Astropart. Phys. **2018**, 019 (2018), arXiv:1708.00492 [astro-ph.CO].

[17] P. McDonald, Journal of Cosmology and Astro-Particle Physics **2009**, 026 (2009), arXiv:0907.5220 [astro-ph.CO].

[18] C. Bonvin, L. Hui, and E. Gaztañaga, Phys. Rev. D **89**, 083535 (2014), arXiv:1309.1321 [astro-ph.CO].

[19] C. Bonvin and P. Fleury, J. Cosmology Astropart. Phys. **2018**, 061 (2018), arXiv:1803.02771 [astro-ph.CO].

[20] C. Bonvin, F. Oliveira Franco, and P. Fleury, J. Cosmology Astropart. Phys. **2020**, 004 (2020), arXiv:2004.06457 [astro-ph.CO].

[21] M.-A. Breton, Y. Rasera, A. Taruya, O. Lacombe, and S. Saga, MNRAS **483**, 2671 (2019), arXiv:1803.04294 [astro-ph.CO].

[22] S. Saga, A. Taruya, M.-A. Breton, and Y. Rasera, MNRAS **498**, 981 (2020), arXiv:2004.03772 [astro-ph.CO].

[23] S. Saga, A. Taruya, M.-A. Breton, and Y. Rasera, arXiv e-prints , arXiv:2109.06012 (2021), arXiv:2109.06012 [astro-ph.CO].

[24] F. Beutler and E. Di Dio, J. Cosmology Astropart. Phys. **2020**, 048 (2020), arXiv:2004.08014 [astro-ph.CO].

[25] S. Alam, H. Zhu, R. A. C. Croft, S. Ho, E. Giusarma, and D. P. Schneider, MNRAS **470**, 2822 (2017), arXiv:1709.07855 [astro-ph.CO].

[26] R. Wojtak, S. H. Hansen, and J. Hjorth, Nature **477**, 567 (2011), arXiv:1109.6571 [astro-ph.CO].

[27] I. Sadeh, L. L. Feng, and O. Lahav, Phys. Rev. Lett. **114**, 071103 (2015), arXiv:1410.5262 [astro-ph.CO].

[28] P. Jimeno, T. Broadhurst, J. Coupon, K. Umetsu, and

* shohei.saga@obspm.fr

[1] C. M. Will, *Theory and Experiment in Gravitational Physics*, 2nd ed. (Cambridge University Press, 2018).

[2] R. V. Pound and G. A. Rebka, Phys. Rev. Lett. **3**, 439 (1959).

[3] R. V. Pound and J. L. Snider, Physical Review **140**, 788 (1965).

[4] R. F. C. Vessot, M. W. Levine, E. M. Mattison, E. L. Blomberg, T. E. Hoffman, G. U. Nystrom, B. F. Farrel, R. Decher, P. B. Eby, and C. R. Baugher, Phys. Rev. Lett. **45**, 2081 (1980).

[5] T. P. Krisher, J. D. Anderson, and J. K. Campbell, Phys. Rev. Lett. **64**, 1322 (1990).

[6] J. C. Lopresto, C. Schrader, and A. K. Pierce, ApJ **376**, 757 (1991).

[7] J. I. González Hernández, R. Rebolo, L. Pasquini, G. Lo Curto, P. Molaro, E. Caffau, H. G. Ludwig, M. Steffen, M. Esposito, A. Suárez Mascareño, B. Toledo-Padrón, R. A. Probst, T. W. Hänsch, R. Holzwarth, A. Manescau, T. Steinmetz, T. Udem, and T. Wilken, A&A **643**, A146 (2020), arXiv:2009.10558 [astro-ph.SR].

[8] N. Leefer, C. T. M. Weber, A. Cingöz, J. R. Torgerson, and D. Budker, Phys. Rev. Lett. **111**, 060801 (2013), arXiv:1304.6940 [physics.atom-ph].

R. Lazkoz, MNRAS **448**, 1999 (2015), arXiv:1410.6050 [astro-ph.CO].

[29] C. T. Mpetha, C. A. Collins, N. Clerc, A. Finoguenov, J. A. Peacock, J. Comparat, D. Schneider, R. Capasso, S. Damsted, K. Furnell, A. Merloni, N. D. Padilla, and A. Saro, MNRAS **503**, 669 (2021), arXiv:2102.11156 [astro-ph.CO].

[30] J. Yoo, Phys. Rev. D **82**, 083508 (2010), arXiv:1009.3021 [astro-ph.CO].

[31] A. Challinor and A. Lewis, Phys. Rev. D **84**, 043516 (2011), arXiv:1105.5292 [astro-ph.CO].

[32] C. Bonvin and R. Durrer, Phys. Rev. D **84**, 063505 (2011), arXiv:1105.5280 [astro-ph.CO].

[33] N. Kaiser, MNRAS **227**, 1 (1987).

[34] J. F. Navarro, C. S. Frenk, and S. D. M. White, ApJ **462**, 563 (1996), arXiv:astro-ph/9508025 [astro-ph].

[35] H. Zhao, J. A. Peacock, and B. Li, Phys. Rev. D **88**, 043013 (2013), arXiv:1206.5032 [astro-ph.CO].

[36] H. Zhu, S. Alam, R. A. C. Croft, S. Ho, and E. Giusarma, MNRAS **471**, 2345 (2017), arXiv:1709.07859 [astro-ph.CO].

[37] E. Di Dio and U. Seljak, J. Cosmology Astropart. Phys. **2019**, 050 (2019), arXiv:1811.03054 [astro-ph.CO].

[38] C. Hikage, R. Mandelbaum, M. Takada, and D. N. Spergel, MNRAS **435**, 2345 (2013), arXiv:1211.1009 [astro-ph.CO].

[39] Z. Yan, N. Raza, L. Van Waerbeke, A. J. Mead, I. G. McCarthy, T. Tröster, and G. Hinshaw, MNRAS **493**, 1120 (2020), arXiv:1912.06663 [astro-ph.CO].

[40] E. Komatsu, K. M. Smith, J. Dunkley, C. L. Bennett, B. Gold, G. Hinshaw, N. Jarosik, D. Larson, M. R. Nolta, L. Page, D. N. Spergel, M. Halpern, R. S. Hill, A. Kogut, M. Limon, S. S. Meyer, N. Odegard, G. S. Tucker, J. L. Weiland, E. Wollack, and E. L. Wright, ApJS **192**, 18 (2011), arXiv:1001.4538 [astro-ph.CO].

[41] H.-J. Seo and D. J. Eisenstein, ApJ **598**, 720 (2003), arXiv:astro-ph/0307460 [astro-ph].

[42] A. Taruya, S. Saito, and T. Nishimichi, Phys. Rev. D **83**, 103527 (2011), arXiv:1101.4723 [astro-ph.CO].

[43] Z. Lukić, D. Reed, S. Habib, and K. Heitmann, ApJ **692**, 217 (2009), arXiv:0803.3624 [astro-ph].

[44] R. K. Sheth and G. Tormen, MNRAS **308**, 119 (1999), arXiv:astro-ph/9901122 [astro-ph].

[45] C. Bonvin, L. Hui, and E. Gaztanaga, J. Cosmology Astropart. Phys. **2016**, 021 (2016), arXiv:1512.03566 [astro-ph.CO].

[46] A. Hall and C. Bonvin, Phys. Rev. D **95**, 043530 (2017), arXiv:1609.09252 [astro-ph.CO].

[47] A. Aghamousa *et al.* (DESI), arXiv e-prints , arXiv:1611.00036 (2016), arXiv:1611.00036 [astro-ph.IM].

[48] R. Laureijs *et al.* (Euclid), arXiv e-prints , arXiv:1110.3193 (2011), arXiv:1110.3193 [astro-ph.CO].

[49] M. Takada, R. S. Ellis, M. Chiba, J. E. Greene, H. Aihara, N. Arimoto, K. Bundy, J. Cohen, O. Doré, G. Graves, J. E. Gunn, T. Heckman, C. M. Hirata, P. Ho, J.-P. Kneib, O. Le Fèvre, L. Lin, S. More, H. Murayama, T. Nagao, M. Ouchi, M. Seiffert, J. D. Silverman, L. Sodré, D. N. Spergel, M. A. Strauss, H. Sugai, Y. Suto, H. Takami, and R. Wyse, PASJ **66**, R1 (2014), arXiv:1206.0737 [astro-ph.CO].

[50] D. J. Bacon *et al.* (SKA), PASA **37**, e007 (2020), arXiv:1811.02743 [astro-ph.CO].

[51] J. W. Brault, *The Gravitational Red Shift in the Solar Spectrum.*, Ph.D. thesis, PRINCETON UNIVERSITY. (1962).

[52] J. L. Snider, Phys. Rev. Lett. **28**, 853 (1972).

[53] R. E. Jenkins, AJ **74**, 960 (1969).

[54] R. F. C. Vessot and M. W. Levine, General Relativity and Gravitation **10**, 181 (1979).

[55] J. P. Turneaure, C. M. Will, B. F. Farrell, E. M. Mattison, and R. F. C. Vessot, Phys. Rev. D **27**, 1705 (1983).

[56] A. Godone, C. Novero, and P. Tavella, Phys. Rev. D **51**, 319 (1995).

[57] A. Bauch and S. Weyers, Phys. Rev. D **65**, 081101 (2002).

[58] N. Ashby, T. P. Heavner, S. R. Jefferts, T. E. Parker, A. G. Radnaev, and Y. O. Dudin, Phys. Rev. Lett. **98**, 070802 (2007).